

# Over-the-Air Computation Systems: Optimization, Analysis and Scaling Laws

Wanchun Liu, *Member, IEEE*, and Xin Zang

**Abstract**— For future Internet of Things (IoT)-based Big Data applications (e.g., smart cities/transportation), wireless data collection from ubiquitous massive smart sensors with limited spectrum bandwidth is very challenging. On the other hand, to interpret the meaning behind the collected data, it is also challenging for edge fusion centers running computing tasks over large data sets with limited computation capacity. To tackle these challenges, by exploiting the superposition property of a multiple-access channel and the functional decomposition properties, the recently proposed technique, over-the-air computation (AirComp), enables an effective joint data collection and computation from concurrent sensor transmissions. In this paper, we focus on a single-antenna AirComp system consisting of  $K$  sensors and one receiver (i.e., the fusion center). We consider an optimization problem to minimize the computation mean-squared error (MSE) of the  $K$  sensors' signals at the receiver by optimizing the transmitting-receiving (Tx-Rx) policy, under the peak power constraint of each sensor. Although the problem is not convex, we derive the computation-optimal policy in closed form. Also, we comprehensively investigate the ergodic performance of AirComp systems in terms of the average computation MSE and the average power consumption under Rayleigh fading channels with different Tx-Rx policies. For the computation-optimal policy, we prove that its average computation MSE has a decay rate of  $O(1/\sqrt{K})$ , and our numerical results illustrate that the policy also has a vanishing average power consumption with the increasing  $K$ , which jointly show the computation effectiveness and the energy efficiency of the policy with a large number of sensors.

**Index Terms**—Wireless sensor networks, over-the-air computation, remote estimation, mean-squared error, optimal power allocation, scaling-law analysis.

## I. INTRODUCTION

Under the fast development of wireless communication, networking, data collection and storage, the era of Big Data has arrived [1]. According to a recent DOMO technical report [2], more than 2 quintillion bytes of data are created every day, and about 1.7 megabytes of data will be created every second per single person on earth by 2020. Also, the Internet of Things (IoT), which connect smart devices that interact with each other and collect all kinds of data, is exponentially growing from 2 billion devices in 2006 to a predicted 200 billion by 2020, and will be one of the primary drivers of data explosion [3]. How to effectively collect and leverage Big Data and interpret the meaning behind it have attracted much attention in the areas of public health, manufacturing, agriculture and farming, energy, transportation, supply chain management and logistics.

The authors are with School of Electrical and Information Engineering, The University of Sydney, Australia. Emails: {wanchun.liu, xin.zang}@sydney.edu.au.

In such IoT-based Big Data applications (e.g., smart cities), wireless data collection from ubiquitous massive smart sensors/devices with limited spectrum bandwidth is very challenging, especially when the data needs to be dealt in a timely manner. On the other hand, due to a large number of data sources, we do not care much about the value of each individual data source anymore, but shift our focus on the fusion of massive data and unleash its power, which is actually a computing problem. The computation of a large amount of data is also challenging for edge devices with limited computation capacity.

To tackle these challenges, the technique, over-the-air computation (AirComp), has been developed to enable an efficient data-fusion of sensing data from many concurrent sensor transmissions by leveraging the inherent broadcast nature of wireless communications and the application of a beautiful mathematical tool in function representation [4].

### A. What is AirComp?

1) *Preliminaries*: Assume an ideal multiple-access channel (MAC) of  $K$  sensors with the signal-superposition property that

$$r = \sum_{k=1}^K u_k, \quad (1)$$

where  $u_k$  is the transmitted signal of sensor  $k$  and  $r$  is the received signal at the receiver.

Consider  $K$  wireless smart sensors, each having a measurement signal  $s_k \in \mathbb{R}, \forall k \in \{1, \dots, K\}$ , and a  $K$ -variate computing task (e.g., sum, multiplication and arithmetic/geometric mean)  $\phi: \mathbb{R}^K \rightarrow \mathbb{R}$  at a designated receiver. By using a mathematical property in the area of theoretical computer science that every real-valued multivariate function is representable in its nomographic form as a function of a finite sum of univariate functions [4], there always exists a set of pre-processing functions  $\psi_k: \mathbb{R} \rightarrow \mathbb{R}, \forall k \in \{1, \dots, K\}$  and a post-processing function  $\varphi: \mathbb{R} \rightarrow \mathbb{R}$  such that

$$\phi(s_1, \dots, s_K) = \varphi \left( \sum_{k=1}^K \psi_k(s_k) \right). \quad (2)$$

2) *The Brief Idea*: Based on (1) and (2), the overall idea of AirComp proposed in [5, 6] is to let each sensor pre-process its own signal and send  $u_k = \psi_k(s_k)$  to the receiver simultaneously, and the receiver processes the received sum of signals  $\sum_{k=1}^K \psi_k(s_k)$  with function  $\varphi(\cdot)$  and thus obtains the desired computation of  $K$  sensors' measurement signals  $\phi(s_1, \dots, s_K)$ . Therefore, the transmission and computation

of a large number of sensors' signals of an AirComp system is completed in one single time slot (i.e., in a symbol level) in contrast to an intuitive one-by-one-transmit-then-compute protocol. In other words, AirComp effectively integrates communication and computation by harnessing interference for computing [6]. Moreover, the receiver's original computation task  $\phi(\cdot)$  of processing  $K$  signals has been decomposed into  $(K+1)$  small tasks  $\{\psi_1(\cdot), \dots, \psi_K(\cdot), \varphi(\cdot)\}$ , and each sensor or the receiver only needs to take one lightweight task with only one signal to be processed. In this way, the computation complexity of the receiver is significantly reduced, especially when  $K$  is large.

3) *Use Cases*: In addition to smart-city applications, e.g., using unmanned aerial vehicles for real-time data computation and collection from sensors embedded in ground vehicles, buildings and other infrastructures, AirComp has been developed and applied in two important emerging mobile applications with highly integrated communication and computation tasks:

- Over-the-air consensus. For example, in drone swarming [7] and connected car platooning [8] applications, each node concurrently sends its current states including velocity and acceleration in real-time, while the central controller can receive and then compute the average current states of the mobile nodes and generate control commands to drive each node approaching to a consensus status [9].
- Wireless distributed machine learning. In wireless machine learning applications that adopt distributed stochastic gradient descent algorithms for model training, each mobile user calculates the gradient of its local cost function of its own data set in terms of the model parameters and concurrently sends it to the parameter server (i.e., a base station), which then computes a weighted average of the gradients and broadcast it to the mobile users for further iteration until convergence [10–12].

## B. Previous Work

The research of AirComp mostly focuses on two aspects: the pre-processing and post-processing functions design in (2), and the analysis of the impact of practical wireless MAC (rather than the ideal one in (1)) on the performance of AirComp and the transceiver design issues for reducing the impact. For the former, the theoretical properties and how to design the pre- and post-processing functions with a given multi-variable target function  $\phi(\cdot)$  (e.g. geometric mean) have been extensively investigated in [5, 6, 13, 14]. For the latter, the computation of the sum of pre-processed signals in (1),  $\sum_{k=1}^K u_k$ , is not perfect due to the non-zero receiver noise and unequal channel coefficients, and hence a key design target is to make the computation distortion of the sum of signals as small as possible. For a multi-antenna AirComp system, an optimization problem of transmitting and receiving beamforming design was considered to minimize the computation distortion [15], based on which a wireless-powered AirComp system was studied in [16]. Also, the effect

of the lack of synchronization between different sensors and the imperfect channel estimation on the distortion of the sum of signals were studied in [5] and [17], respectively.

We would note that using the signal-superposition property of a MAC for direct information fusion from multiple terminals is not new and it has been successfully utilized in solving the classic central estimation officer (CEO) problem in the area of remote estimation of traditional wireless sensor networks (WSNs) [18]. In this application, each sensor takes a noisy observation of the same source (a deterministic parameter or a random process), and concurrently sends the uncoded (linearly scaled) signal to the fusion center through a MAC. The fusion center receives the superimposed signals and reconstructs the source signal of interest. The CEO problems of deterministic parameter estimation under single and multiple antenna settings were investigated in [19] and [20, 21], respectively. A CEO problem for Gauss-Markov process estimation was considered in [22]. Although both the traditional CEO and the recent AirComp systems make use of MACs for data fusion, the former only needs to estimate a single-source signal while the latter has to estimate a function of distributed multi-source signals. Thus, the design targets and the optimal solutions of these two problems are fundamentally different.

## C. Contributions and Paper Organization

In this paper, we focus on a baseline single-antenna AirComp system with non-zero receiver noise and unequal channel coefficients, where the sensors send linearly scaled pre-processed signals simultaneously to the receiver, which then linearly scales the received signal as the computing output of the sum of the pre-processed signals.<sup>2</sup> The main contributions of the paper are summarized as follows.

- We consider an optimization problem to minimize the computation mean-squared error (MSE) of the sum of the pre-processed signals at the receiver by optimizing the transmitting-receiving (Tx-Rx) scaling policy, where each sensor has a peak power limit for transmission. Although the problem is not convex, we derive the optimal solution in closed form. We would note that such the type of problem has been considered under a more complicated setting of multi-antenna multi-modal sensing in [15], which, however, only gave a suboptimal solution due to the non-convexity of the problem. When considering the single-antenna and single-modal setting, the solution in [15] degrades to a Tx-Rx scaling policy of a channel-inversion type, which actually leads to a much larger computation MSE than the optimal policy obtained in our paper.

<sup>2</sup>Such the AirComp system actually uses an analog (or coding-free) transmission method. Note that in the area of WSNs and wireless remote estimation/control systems, extensive research has focused on the fusion of analog data instead of encoded digital data (see [19–22], [23–25] and references therein). This is mainly because digital transmission achieves an exponentially worse performance than analog signaling in terms of distortion between the source signal and the recovered signal, which has been proved by pioneer works in [26–28].

- We also investigate a MAC system for distributed remote estimation, which is closely related to the AirComp system. In this system, each sensor sends its scaled measurement signal to the receiver simultaneously, which then needs to recover each sensor's signal as accurately as possible. We formulate and solve an optimization problem to minimize the sum of the estimation MSE of each sensor's signal at the receiver by optimizing the Tx-Rx scaling policy, under the peak power constraint of each sensor.<sup>3</sup> Interestingly, such the estimation problem of the MAC system is a sum-of-MSE problem, while the AirComp system introduces an MSE-of-sum problem. We also prove the condition under which the optimal Tx-Rx scaling policies of the MAC and AirComp systems are equivalent to each other.
- We investigate the ergodic performance of AirComp systems in terms of the average computation MSE and the average power consumption under Rayleigh fading channels. We comprehensively study the scaling laws of the average computation MSE and the average power consumption of different Tx-Rx scaling policies with respect to the number of sensors  $K$ . Also, we define two types of policies: the computation-effective policy, which has a vanishing average computation MSE, and the energy-efficient policy, which has a vanishing average power consumption, with the increasing number of sensors  $K$ . Since there is a tradeoff in policy design between the computation effectiveness and the energy efficiency of the AirComp system, it is not clear whether there exists a policy that is both computation-effective and energy-efficient. We rigorously prove the existence of such the type of policy. Moreover, for the computation-optimal policy, we prove that the policy is a computation-effective one and its average computation MSE has a decay rate of  $O(1/\sqrt{K})$ . Our numerical results show that the policy is also energy-efficient.

The remainder of the paper is organized as follows: Sec. II describes the AirComp system and formulate a computation-MSE-minimization problem. In Sec. III, we solve the optimization problem and obtain the computation-optimal Tx-Rx scaling policy. In Sec. IV, we study a MAC-based remote estimation problem which is closely related to the AirComp problem, and then compare the optimal policies of the two problems. In Sec. V, the ergodic performance of the AirComp system with different Tx-Rx scaling policies are investigated in terms of the average computation MSE and the average power consumption. Sec. VI numerically evaluates the performance of AirComp systems with different policies. Finally, Sec. VII concludes this work.

Notations: For two functions  $g(x)$  and  $f(x)$ , the notation  $g(x) = O(f(x))$  and  $g(x) = o(f(x)), x \rightarrow \infty$ , means

<sup>3</sup>Note that the research of traditional MAC is mostly focused on rate-centric systems, where the design target is commonly to maximize the achievable sum rate of the  $K$  users [29–31]. For estimation-centric MAC, the optimization problem for minimizing the sum of estimation MSEs was considered under the sum power constraint in [32].

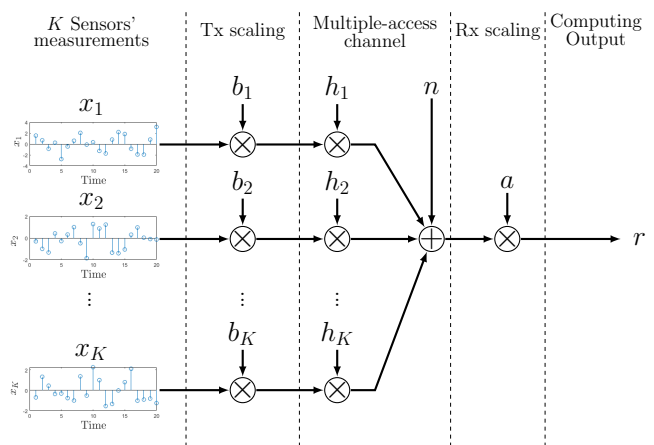


Fig. 1: Illustration of the AirComp system.

that  $\limsup_{x \rightarrow \infty} g(x)/f(x) < \infty$  and  $\lim_{x \rightarrow \infty} g(x)/f(x) = 0$ , respectively. We denote  $f(x) \sim g(x)$  if  $g(x) = O(f(x))$  and  $f(x) = O(g(x))$ .  $\mathbb{R}$  and  $\mathbb{R}_0$  denote the set of real number and the set of non-negative real number, respectively.  $\mathbb{N}$  denotes the set of positive integers.

## II. SYSTEM MODEL

We consider a  $K$ -sensor single-antenna AirComp system as illustrated in Fig. 1. Each sensor's pre-processed signal  $x_k \in \mathbb{R}, \forall k \in \{1, \dots, K\}$ , is scaled by its Tx-scaling factor  $b_k \in \mathbb{C}$  and sent to the receiver simultaneously through a MAC. The receiver applies a Rx-scaling factor  $a$  to the received signal as the computing output of the sum of the  $K$  sensors' signals as

$$r = a \left( \sum_{k=1}^K h_k b_k x_k + n \right), \quad (3)$$

where  $h_k \in \mathbb{C}$  is the channel coefficient between sensor  $k$  to the receiver and  $n$  is the additive white Gaussian noise (AWGN). It is assumed that the channel coefficients are known by both the sensors and the receiver, and the sensors' transmissions are well synchronized [10–13, 15].<sup>4</sup> We assume that the pre-processed signal  $x_k \in [-v, v] \subset \mathbb{R}, \forall k \in \{1, \dots, K\}$ , is zero-mean with normalized variance, and is independent with the others [15, 16].

The computation distortion of the ideal sum of the signals  $\sum_{k=1}^K x_k$  is measured by its mean-squared error (MSE) as

$$\text{MSE} = \mathbb{E} \left[ \left| r - \sum_{k=1}^K x_k \right|^2 \right], \quad (4)$$

where the expectation is taken with respect to the randomness of the original signals  $\{x_k\}$  and the receiver noise  $n$ . Substituting (3) into (4), the computation MSE of the AirComp system is rewritten as

$$\text{MSE} = \sum_{k=1}^K |ah_k b_k - 1|^2 + \sigma^2 |a|^2. \quad (5)$$

<sup>4</sup>The effects of imperfect channel estimation and synchronization have been discussed in [5, 6, 17].

Considering a peak power constraint of each sensor's transmission,  $P'$ , we have

$$\max_{x_k \in [-v, v]} |b_k x_k|^2 = |b_k|^2 v^2 \leq P' \iff |b_k|^2 \leq P, \forall k$$

where  $P \triangleq P'/v^2$ .

Since the pre-processed signal  $x_k$  has a normalized variance, the average transmission power of sensor  $k$  is  $E[|b_k x_k|^2] = |b_k|^2$ . Thus, the power consumption of the  $K$ -sensor AirComp system is

$$\text{PW} \triangleq \sum_{k=1}^K |b_k|^2. \quad (6)$$

Given the channel coefficients  $\{h_k\}$ , the MSE-minimization problem in terms of the Tx-Rx scaling policy under the peak power constraint is formulated as

$$\min_{a, \{b_k\}} \text{MSE} \quad (7a)$$

$$\text{subject to } |b_k|^2 \leq P, \forall k. \quad (7b)$$

From the target function definition in (5), given the complex Rx-scaling factor  $a$  and the channel coefficient  $h_k$ , sensor  $k$  is always able to adjust the phase of its Tx-scaling factor  $b_k$  for phase compensation without changing its magnitude such that the term  $ah_k b_k$  is real and non-negative and thus minimizes  $|ah_k b_k - 1|$  in (5). In this sense, only the magnitudes of  $a$ ,  $\{h_k\}$  and  $\{b_k\}$  have effect on achieving the minimum MSE in problem (7). Therefore, without loss of generality, we set  $a, h_k \in \mathbb{R}_0$ , and  $b_k \in [0, \sqrt{P}]$ ,  $\forall k$ , in the rest of the paper.

Problem (7) is non-convex as the target function (7a) is not a convex function of  $a$  and  $\{b_k\}$ . However, the problem is convex when  $a$  or  $\{b_k\}$  is fixed. Thus, an intuitive method for solving the problem can be the alternating-direction method, i.e., fixing  $\{b_k\}$  that satisfies (7b) and solving the optimal  $a$ , and then in turn solving the optimal  $\{b_k\}$  with the optimal  $a$ , and so on. However, such the algorithm may not guarantee the convergence to a global optimal solution.

In the following section, we derive the closed-form Tx-Rx scaling policy of problem (7), which is named as the computation-optimal policy.

### III. COMPUTATION-OPTIMAL AIRCOMP SYSTEM

#### A. Computation-Optimal Policy

Without loss of generality, we assume the channel coefficients have the property that  $0 \triangleq h_0 < h_1 \leq h_2 \leq \dots \leq h_K < h_{K+1} \triangleq \infty$ . We then introduce a sequence of  $(K+1)$  disjoint intervals  $\{\mathcal{S}_k\}$  that covers  $\mathbb{R}_0$  as

$$\mathcal{S}_k \triangleq \begin{cases} \left( \frac{1}{h_1 \sqrt{P}}, \infty \right), & k = 0, \\ \left( \frac{1}{h_{k+1} \sqrt{P}}, \frac{1}{h_k \sqrt{P}} \right], & k = 1, \dots, K-1, \\ \left[ 0, \frac{1}{h_K \sqrt{P}} \right], & k = K, \end{cases}$$

which is illustrated in Fig. 2(a).

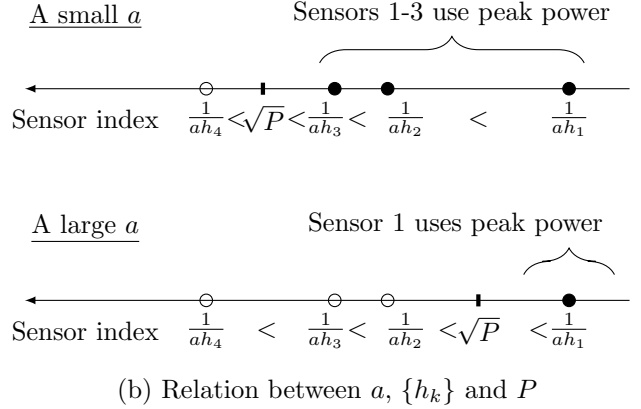
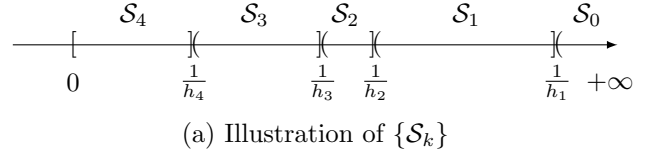


Fig. 2: Illustration of  $\{\mathcal{S}_k\}$  and the relation between  $a$ ,  $\{h_k\}$  and  $P$ , where  $K = 4$ .

From (5), it is clear that if  $a \in \mathcal{S}_i$ , where  $i$  is named as the *critical number* of the Tx-Rx scaling policy,  $|ah_k b_k - 1|^2$  monotonically decreases with the increasing of  $b_k \in [0, \sqrt{P}]$ ,  $\forall k \in \{1, \dots, i\}$ ; while  $|ah_k b_k - 1|^2$  is minimized and equal to zero when  $b_k = 1/(ah_k) < \sqrt{P}$ ,  $\forall k \in \{i+1, \dots, K\}$ , as illustrated in Fig. 2(b). Thus, we have the following result.

**Lemma 1a.** If the Rx-scaling factor  $a \in \mathcal{S}_i$ ,  $i = 0, 1, \dots, K$ , the optimal Tx-scaling factors  $\{b_k\}$  are given as

$$b_k = \begin{cases} \sqrt{P}, & 1 \leq k \leq i \\ \frac{1}{ah_k}, & i < k \leq K, \end{cases} \quad (8)$$

**Remark 1.** Lemma 1a shows that the critical number  $i$  indicates the number of sensors using the maximum power for transmission. Also, the Tx-scaling factors of the computation-optimal policy has a switching structure, i.e.,  $i$  sensors with the smallest channel coefficients have to use the maximum power for transmission, while the power consumption of the rest  $(K-i)$  sensors is of a channel-inversion type. Also, as illustrated in Fig. 2(b), more sensors have to use the maximum power for transmission if the Rx-scaling factor is small.

Using Lemma 1a, since  $\sum_{k=i+1}^K |ah_k b_k - 1|^2 = 0$ , the target function of problem (7) can be rewritten as

$$\text{MSE} = \sum_{k=1}^i |ah_k \sqrt{P} - 1|^2 + \sigma^2 |a|^2, a \in \mathcal{S}_i, \quad (9)$$

which is a quadratic function of the Rx-scaling factor  $a$ . The following result is obtained directly as

**Lemma 1b.** If the Rx-scaling factor  $a \in \mathcal{S}_i$ ,  $i = 0, 1, \dots, K$ , the optimal Rx-scaling factor is given as

$$a_i = \begin{cases} \left( \frac{1}{h_{i+1}\sqrt{P}} \right)^+, & \text{if } g_i < \mathcal{S}_i \\ g_i, & \text{if } g_i \in \mathcal{S}_i \\ \frac{1}{h_i\sqrt{P}}, & \text{if } g_i > \mathcal{S}_i \end{cases} \quad (10)$$

where the operator  $(u)^+$  indicates approaching to the real number  $u$  from right side, and with a bit abuse of notation,  $g_i > \mathcal{S}_i$  and  $g_i < \mathcal{S}_i$  denote  $g_i \leq \frac{1}{h_{i+1}\sqrt{P}}$  and  $g_i > \frac{1}{h_{i+1}\sqrt{P}}$ , respectively, where  $g_i$  is the optimal solution of (9) without the constraint  $a \in \mathcal{S}_i$  and is given as

$$g_i \triangleq \begin{cases} 0, & i = 0 \\ \frac{\sqrt{P} \sum_{k=1}^i h_k}{\sigma^2 + P \sum_{k=1}^i h_k^2}, & i = 1, \dots, K. \end{cases} \quad (11)$$

Based on Lemma 1b, if  $g_i \notin \mathcal{S}_i$ , i.e., the first and the last cases in (10), the following property reveals how to find a better Rx-scaling factor  $a$  leading to a smaller MSE.

**Lemma 1c.** If  $g_i < \mathcal{S}_i$  and  $i < K$ , there exists  $a \in \mathcal{S}_{i+1}$  that achieves a smaller MSE than  $a_i$ . If  $g_i > \mathcal{S}_i$  and  $i > 0$ , there exists  $a \in \mathcal{S}_{i-1}$  that achieves a smaller MSE than  $a_i$ .

*Proof.* For the first case, it is not hard to see  $a = \frac{1}{h_{i+1}\sqrt{P}} \in \mathcal{S}_{i+1}$  leads to a smaller MSE due to the continuity of the target function (9). For the second case, assuming that  $g_i \in \mathcal{S}_{i'}$  and  $i' < i$ , since the quadratic function (9) monotonically decreases and then increases, there exists  $a' \in \mathcal{S}_{i-1}$  such that

$$\begin{aligned} \sum_{k=1}^{i-1} \left| a' h_k \sqrt{P} - 1 \right|^2 + \sigma^2 |a'|^2 &\leq \sum_{k=1}^i \left| a' h_k \sqrt{P} - 1 \right|^2 + \sigma^2 |a'|^2 \\ &< \sum_{k=1}^i \left| a h_k \sqrt{P} - 1 \right|^2 + \sigma^2 |a|^2, \end{aligned} \quad (12)$$

where the first term in (12) is the minimum MSE achieved by  $a' \in \mathcal{S}_{i-1}$  from Lemma 1a, completing the proof. ■

Jointly using Lemma 1b and Lemma 1c, it can be obtained that

**Corollary 1.** The optimal Rx-scaling factor  $a \notin \mathcal{S}_0$ , i.e., in order to achieve the minimum MSE, at least one sensor needs to transmit with the maximum power.

Based on Lemma 1a and Lemma 1b, to find the optimal Rx-scaling factor  $a^*$ , we only need to know the optimal critical number  $i^*$ , i.e.,  $a^* = a_{i^*} \in \mathcal{S}_{i^*}$ , which is the most important part for solving the problem. Thus, problem (7) is reformulated as

$$\min_{1 \leq i \leq K} \text{MSE}_i \triangleq \sum_{k=1}^i \left| a_i h_k \sqrt{P} - 1 \right|^2 + \sigma^2 |a_i|^2 \quad (13)$$

subject to (10).

From Lemma 1b, since  $a_i$  depends on  $g_i, \forall i \in \{1, \dots, K\}$ , the optimal  $a, a^* \in \{a_1, \dots, a_K\}$ , depends on the sequence

$\{g_i\}$ . In what follows, we introduce the technical lemmas of the properties of  $\{g_i\}$ , which will be utilized for finding  $a^*$ .

**Lemma 2a** (Switching structure). If  $g_i \in \mathcal{S}_i$ , then

$$\begin{cases} g_{i+1} > \mathcal{S}_{i+1}, & \text{if } i < K, \\ g_{i-1} < \mathcal{S}_{i-1}, & \text{if } i > 0. \end{cases} \quad (14)$$

*Proof.* (14) can be verified by using the definition of  $g_i$  in (11) and the property that  $\frac{a}{b} \geq \frac{c}{d} \iff \frac{a+c}{b+d} \geq \frac{c}{d}$ , where  $a, b, c, d > 0$ . The following lemmas can be verified using the similar steps, and the proofs are omitted for brevity. ■

**Lemma 2b** (Consistency). If  $g_i < \mathcal{S}_i$  and  $i > 0$ , then  $g_{i-1} < \mathcal{S}_{i-1}$ . If  $g_i > \mathcal{S}_i$  and  $i < K$ , then  $g_{i+1} > \mathcal{S}_{i+1}$ .

**Lemma 2c** (Monotonicity). If  $g_i < \mathcal{S}_i$  and  $i < K$ , then  $g_i \leq g_{i+1}$ . If  $g_i > \mathcal{S}_i$  and  $i > 0$ , then  $g_i \leq g_{i-1}$ .

Jointly using Lemma 2a and Lemma 2c, it shows the unimodality of the sequence  $\{g_i\}$ , i.e., there exists  $i^*$  such that  $g_i$  monotonically increases and decreases with  $i$  for all  $i \leq i^*$  and  $i \geq i^*$ , respectively. Then, using Lemma 2a and Lemma 2b together with Lemma 1c, the unimodality of the sequence  $\{-\text{MSE}_i\}$  in (13) can be easily verified, as  $\text{MSE}_i$  monotonically decreases and increases with  $i$  for  $i \leq i^*$  and  $i \geq i^*$ , respectively. Therefore, the optimal Tx-Rx scaling policy is given below.

**Theorem 1** (Computation-optimal policy). The optimal critical number of problem (7) is

$$i^* = \arg \max_{1 \leq i \leq K} g_i.$$

The optimal Rx-scaling factor  $a^*$  is  $a_{i^*}$  by taking  $i^*$  into (10). The optimal Tx-scaling factors  $\{b_k^*\}$  are obtained by taking  $i^*$  into (8).

We note that this result is independently arrived at [33] with a different proof.

As a consequence of Theorem 1, the computation MSE and the power consumption induced by the computation-optimal policy is obtained below.

**Proposition 1.** The minimum computation MSE of the AirComp system under the peak power constraint is

$$\text{MSE}^* = \sum_{k=1}^{i^*} \left( a_{i^*} h_k \sqrt{P} - 1 \right)^2 + \sigma^2 (a_{i^*})^2. \quad (15)$$

The power consumption of the AirComp system induced by the computation-optimal policy is

$$\text{PW} = \sum_{k=1}^K b_k^{*2} = P i^* + \frac{1}{(a_{i^*})^2} \sum_{k=i^*+1}^K \frac{1}{h_k^2}. \quad (16)$$

## B. Benchmark Policies

The computation-optimal policy in Theorem 1 needs to first sort the  $K$  channel coefficients (e.g., using an insertion-sort algorithm), which has a computation complexity of  $O(K^2)$ , and then compute the largest parameter  $g_i$ , which is a non-linear

function of  $i$  channel coefficients. Thus, we also present two intuitive and easy-to-compute benchmark policies of AirComp systems for comparison.

**Definition 1** (Channel-inversion policy). The channel-inversion policy has the critical number  $i = 1$ , i.e., the Rx-scaling factor  $a \in \mathcal{S}_1$ , and the Tx and Rx-scaling factors are give as

$$\begin{aligned} b_k &= \sqrt{P} \frac{h_1}{h_k}, \forall k \\ a &= \frac{1}{\sqrt{P}h_1}. \end{aligned} \quad (17)$$

The channel-inversion policy is commonly considered in the literature of AirComp [15, 16], which guarantees that the computing output  $r$  in (3) is an unbiased estimation of the sum of the original signals, i.e.,

$$\mathbb{E} \left[ r - \sum_{k=1}^K x_k \middle| x_1, \dots, x_K \right] = a \mathbb{E}[n] = 0.$$

**Definition 2** (Energy-greedy policy). The energy-greedy policy always choose the critical number  $i = K$ , i.e., the Rx-scaling factor  $a \in \mathcal{S}_K$ , and the Tx and Rx-scaling factors according to Lemma 1a and Lemma 1b are give as

$$b_k = \sqrt{P}, \forall k, \quad (18a)$$

$$a = \min \left\{ \frac{1}{\sqrt{P}h_K}, \frac{\sqrt{P} \sum_{k=1}^K h_k}{\sigma^2 + P \sum_{k=1}^K h_k^2} \right\}. \quad (18b)$$

The energy-greedy policy requires all the sensors to always transmit with the maximum power regardless of the channel coefficients. Since the optimal critical number of an AirComp system,  $i^*$ , usually takes value between 1 and  $K$ , the channel-inversion policy and the energy-greedy policy can be treated as two extreme cases.

#### IV. AIRCOMP SYSTEM VERSUS TRADITIONAL MAC SYSTEM

In this section, we consider a remote estimation problem based on a MAC system, which is closely related to the AirComp problem. The MAC system consists of  $K$  sensors and one receiver, where the receiver has to recover every sensor's signal  $x_k, \forall k \in \{1, \dots, K\}$ . The sensors adopt the coding-free transmission method same as the AirComp system, i.e., each of the  $K$  sensors scales its measurement signal by the Tx-scaling factor  $\tilde{b}_k$  and simultaneously sends it to the receiver. Then, the receiver estimates each of the original signal by linearly scaling the received signal with the Rx-scaling factor  $\tilde{a}_k, \forall k \in \{1, \dots, K\}$ . The estimated sensor  $k$ 's signal is given as

$$r_k = \tilde{a}_k \left( \sum_{k=1}^K h_k \tilde{b}_k x_k + n \right), \forall k \in \{1, \dots, K\}.$$

With a bit abuse of notation, the estimation MSE of sensor  $k$  is denoted and obtained as

$$\begin{aligned} \text{MSE}_k &\triangleq \mathbb{E} [|r_k - x_k|^2] \\ &= (\tilde{a}_k h_k \tilde{b}_k - 1)^2 + \tilde{a}_k^2 \sum_{j \in \{1, \dots, K\} \setminus k} (h_j \tilde{b}_j)^2 + \tilde{a}_k^2 \sigma^2. \end{aligned} \quad (19)$$

##### A. Optimal Sum of MSE

We aim to design the optimal Tx-Rx scaling policy to minimize the sum of the estimation MSEs of the  $K$  sensors' signals under the individual power constraint, and have the following problem:

$$\min_{\{\tilde{a}_k\}, \{\tilde{b}_k\}} \sum_{k=1}^K \text{MSE}_k \quad (21a)$$

$$\text{subject to } |\tilde{b}_k|^2 \leq P, \forall k. \quad (21b)$$

**Remark 2.** This optimal estimation problem of the MAC system is a sum-of-MSE problem, while the optimization problem of the AirComp system in Sec. III-A can be treated as an MSE-of-sum (signal) problem. Thus, the optimal Tx-Rx scaling policies of the two problems are different in general.

When  $\{\tilde{b}_k\}$  are given and satisfy the constraint (21b), the target function (21a) is a quadratic function of  $\{\tilde{a}_k\}$  and the optimal Rx-scaling factor for sensor  $k$  is obtained directly as

$$\tilde{a}_k = \frac{h_k \tilde{b}_k}{\sigma^2 + \sum_{j=1}^K (h_j \tilde{b}_j)^2}. \quad (22)$$

Taking (22) into (20), we have

$$\text{MSE}_k = 1 - \frac{(h_k \tilde{b}_k)^2}{\sigma^2 + \sum_{j=1}^K (h_j \tilde{b}_j)^2}, \quad (23)$$

and thus

$$\sum_{k=1}^K \text{MSE}_k = K - \frac{\sum_{j=1}^K (h_j \tilde{b}_j)^2}{\sigma^2 + \sum_{j=1}^K (h_j \tilde{b}_j)^2},$$

which is a monotonic decreasing function of  $\{\tilde{b}_k^2\}$ . Therefore, the optimal solution of problem (21) is given below.

**Theorem 2** (Optimal sum-of-MSE policy). The optimal Tx-Rx scaling policy of problem (21) of the MAC system is given as

$$\begin{aligned} \tilde{a}_k^* &= \frac{h_k \sqrt{P}}{\sigma^2 + P \sum_{j=1}^K (h_j)^2}, \forall k \\ \tilde{b}_k^* &= \sqrt{P}, \forall k \end{aligned}$$

**Remark 3** (When the sum-of-MSE problem is equivalent to the MSE-of-sum problem?). Different from the computation-optimal policy of the AirComp system in Theorem 1, where the optimal Tx-scaling factor of each sensor depends on  $K$  channel coefficients, the optimal policy of the MAC system has the identical Tx-scaling factor  $\sqrt{P}$ , i.e., a type of energy-greedy policy that requires each sensor to use the maximum power for transmission.

However, from Theorems 1 and 2, if the sequence  $\{g_i\}$  defined in (11) satisfies the condition

$$g_K = \max_{1 \leq k \leq K} g_k,$$

the optimal Tx-scaling factors of the AirComp system is identical to that of the MAC system, i.e.,  $b_k^* = \tilde{b}_k^* = \sqrt{P}, \forall k$ . Also the optimal Rx-scaling factor of the AirComp system  $a^* = \frac{\sum_{k=1}^K h_k \sqrt{P}}{\sigma^2 + P \sum_{j=1}^K (h_j)^2}$  is equal to the sum of the optimal Rx-scaling factors of the MAC system  $\sum_{k=1}^K \tilde{a}_k^*$ , and thus the estimation of the sum of the signals is equal to the sum of the estimation of each individual signal, i.e.,  $r = \sum_{k=1}^K r_k$ . In this sense, the optimal sum-of-MSE policy is equivalent to the optimal MSE-of-sum policy.

### B. Achievable MSE Region

In addition to the sum of the estimation MSEs of  $K$  sensors' signals, we also care about the capability of the MAC system in providing the estimation quality of the  $K$  sensors, which is captured by the achievable MSE region defined below.

**Definition 3** (Achievable MSE region). Given the channel coefficients  $\{h_k\}$  and the individual power constraint  $P$ , the achievable MSE region of a  $K$ -sensor MAC,  $\mathcal{M}$ , is defined by the set of all tuples  $(\text{MSE}_1, \dots, \text{MSE}_K)$ , where  $\text{MSE}_k$  is defined in (19),  $\tilde{a}_k$  is given in (22), and  $\tilde{b}_k \in [0, \sqrt{P}], \forall k \in \{1, \dots, K\}$ .

Using (23),  $b_k^2$  can be represented by  $\{\text{MSE}_j\}$  as

$$b_k^2 = \frac{\sigma^2}{h_k^2} \frac{1 - \text{MSE}_k}{\sum_{j=1}^K \text{MSE}_j - 1}, \forall k.$$

Since  $b_k^2 \leq P$  and  $\text{MSE}_k \leq 1$  in (23), the achievable MSE region can be derived as below.

**Proposition 2.** The achievable MSE region of a  $K$ -sensor MAC,  $\mathcal{M}$ , satisfies

$$\text{MSE}_k + \frac{Ph_k^2}{\sigma^2} \left( \sum_{j=1}^K \text{MSE}_j - 1 \right) \geq 1, \forall k \quad (24a)$$

$$\text{MSE}_k \leq 1, \forall k. \quad (24b)$$

**Remark 4.** It can be verified that the achievable MSE region (24) is convex, and (24a) and (24b) defines the inner and outer boundaries of the region, respectively, as illustrated in Fig. 3. Specifically, the inner boundary (24a) is achieved by letting the  $k$ th sensor transmit with the maximum power, i.e.,  $b_k^2 = P$ .

From Corollary 1, the computation-optimal policy of the AirComp system assigns at least one sensor using the maximum power for information transmission. Thus, applying the optimal Tx-scaling factors of the AirComp system  $\{b_k^*\}$  to the MAC system, i.e., letting  $\tilde{b}_k = b_k^*, \forall k$ , the achievable MSE tuple  $(\text{MSE}_1, \dots, \text{MSE}_K)$  falls on the inner boundaries of the achievable MSE region  $\mathcal{M}$ . For the optimal Tx-scaling factors of the MAC system, i.e.,  $\tilde{b}_k^* = \sqrt{P}$ , the equalities of the  $K$  constraints (24a) holds, thus the achievable MSE tuple  $(\text{MSE}_1, \dots, \text{MSE}_K)$  is the intersection of the inner boundaries as illustrated in Fig. 3.

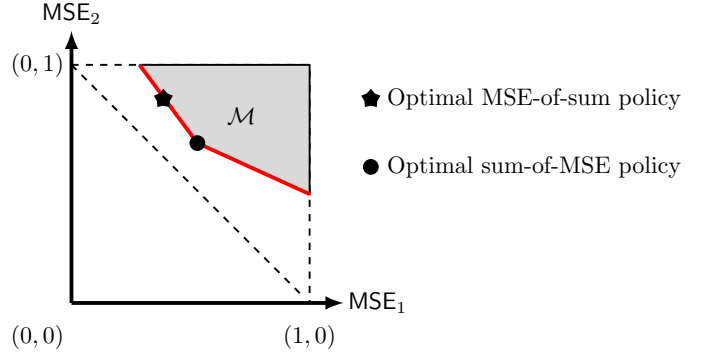


Fig. 3: Achievable MSE region of a two-sensor MAC system.

## V. SCALING LAWS OF AIRCOMP SYSTEMS: COMPUTATION EFFECTIVENESS VERSUS ENERGY EFFICIENCY

In Sec. III, the performance of the AirComp system under instantaneous channel conditions has been investigated. In this section, we focus on the ergodic performance of AirComp systems with different Tx-Rx scaling policies under Rayleigh fading channels, where each channel coefficient  $h_k, \forall k \in \{1, \dots, K\}$ , independently varies with time and has the standard Rayleigh stationary distribution [34]. In particular, we investigate the average computation MSE and the average power consumption of the AirComp system defined below.<sup>5</sup>

**Definition 4.** The average computation MSE and the average power consumption of an AirComp system are defined respectively as  $E[\text{MSE}]/K$  and  $E[\text{PW}]/K$ , where MSE and PW are given in (5) and (6), respectively, and the expectation is taken with respect to  $K$  random channel coefficients.

Thus, the average computation MSE and the average power consumption indicate how the computation accuracy/performance and the total power consumption of the AirComp system scale with the increasing computation load, i.e., the increasing  $K$ .

**Definition 5.** A Tx-Rx scaling policy of the AirComp system is a computation-effective policy iff

$$\lim_{K \rightarrow \infty} \frac{E[\text{MSE}]}{K} = 0.$$

The policy is an energy-efficient policy iff

$$\lim_{K \rightarrow \infty} \frac{E[\text{PW}]}{K} = 0.$$

For a computation-effective policy, the average computation MSE approaches to zero, while for an energy-efficient policy, the average power consumption approaches to zero, with the increasing computation load. Therefore, it is interesting to see whether the benchmark policies (including the

<sup>5</sup>Although the following analysis are for AirComp systems with Rayleigh-distributed channel coefficients, the analysis framework can be applied to the cases with other channel-coefficient distributions.

channel-inversion policy and the energy-greedy policy), and the computation-optimal policy in Sec. III are computation-effective or energy-efficient or both.

In the following analysis, we denote the channel power gains as  $U_k \triangleq h_k^2$ , where  $U_{k_1} \leq U_{k_2}, \forall 1 \leq k_1 \leq k_2 \leq K$ . In other words,  $\{U_k\}$  are the order statistics of  $K$  independent random samples from the standard exponential distributions.

#### A. Benchmark Policy 1: Channel-Inversion Policy

1) *Average Computation MSE*: Taking (17) into (5), the average computation MSE can be derived as

$$\frac{\mathbb{E}[\text{MSE}]}{K} = \frac{1}{K} \mathbb{E} \left[ \frac{\sigma^2}{PU_1} \right]. \quad (25)$$

Using the property of order statistics [35], the probability density function (pdf) of the minimum value of  $K$  sample from the standard exponential distribution is given as

$$f_{U_1}(u_1) = \begin{cases} Ke^{-Ku_1}, & u_1 \geq 0 \\ 0, & u_1 < 0 \end{cases} \quad (26)$$

Thus,  $U_1$  follows an exponential distribution and  $1/U_1$  follows an inverse exponential distribution with the pdf

$$f_{1/U_1}(y) = \exp\left(-\frac{K}{y}\right) \frac{K}{y^2}. \quad (27)$$

Taking (27) into (25), the average computation MSE is calculated as

$$\frac{\mathbb{E}[\text{MSE}]}{K} = \frac{\sigma^2}{P} \frac{1}{K} \int_0^\infty y \exp\left(-\frac{K}{y}\right) \frac{K}{y^2} dy = \infty.$$

Therefore, the channel-inversion method actually leads to a poor computation performance, and we have the following result.

**Corollary 2.** The average computation MSE of the channel-inversion policy is infinite. The policy is not a computation-effective one.

2) *Average Power Consumption*: From (17), the average power consumption is derived as

$$\frac{\mathbb{E}[\text{PW}]}{K} = \frac{P}{K} \left( 1 + \mathbb{E} \left[ \sum_{k=2}^K \frac{U_1}{U_k} \right] \right), \quad (28)$$

where

$$\begin{aligned} & \mathbb{E} \left[ \sum_{k=2}^K \frac{U_1}{U_k} \right] \\ &= \int_{u_1, \dots, u_K} \left( \sum_{k=2}^K \frac{u_1}{u_k} \right) f(u_1, u_2, \dots, u_K) du_1, \dots, du_K, \end{aligned}$$

and  $f(u_1, u_2, \dots, u_K)$  is the joint distribution of  $U_1, \dots, U_K$ . Then, we have the following result.

**Corollary 3.** The average power consumption of the channel-inversion policy is

$$\frac{\mathbb{E}[\text{PW}]}{K} = \frac{P \ln K}{K-1},$$

which has the scaling law as

$$\frac{\mathbb{E}[\text{PW}]}{K} \sim \frac{\ln K}{K}, K \rightarrow \infty.$$

The policy is an energy-efficient one.

*Proof.* See Appendix A ■

#### B. Benchmark Policy 2: Energy-Greedy Policy

1) *Average Computation MSE*: From (18), the Rx-scaling factor of the energy-greedy policy may have the sum of channel coefficients and the sum of channel power gains in the numerator and the denominator, respectively, which makes the analysis of average computation MSE difficult. Thus, we analyze an upper bound the average computation MSE. From Lemma 1b, letting  $a = \frac{1}{\sqrt{Ph_K}}$  always results in an MSE no smaller than that in (18b), and thus we have

$$\begin{aligned} \frac{\mathbb{E}[\text{MSE}]}{K} &\leq \frac{1}{K} \mathbb{E} \left[ \sum_{k=1}^K \left| 1 - \frac{h_k}{h_K} \right|^2 + \frac{\sigma^2}{Ph_K^2} \right] \\ &\leq 1 + \mathbb{E} \left[ \frac{\sigma^2}{PKU_K} \right], \end{aligned} \quad (29)$$

where (29) is due to the fact that  $h_k \leq h_K, \forall k$ .

Again, using the property of order statistics [35], the largest sample of  $K$  standard exponential distribution  $U_K$  has the pdf as

$$f_{U_K}(u_K) = \begin{cases} Ke^{-u_K}(1-e^{-u_K})^{K-1}, & u_K \geq 0 \\ 0, & u_K < 0 \end{cases} \quad (30)$$

Applying (30) onto (29), it is obtained as

$$\begin{aligned} \frac{\mathbb{E}[\text{MSE}]}{K} &\leq 1 + \int_0^\infty \frac{e^{-x}(1-e^{-x})^{K-1}}{x} dx \\ &\leq 1 + \int_0^\infty \frac{e^{-x}(1-e^{-x})}{x} dx \\ &= 1 + \ln 2 < \infty. \end{aligned}$$

Also, it can be directly proved that  $\limsup_{K \rightarrow \infty} \mathbb{E}[\text{MSE}]/K$  is greater than a positive constant by using Theorem 3 from the latter part of the paper. We have the following result.

**Corollary 4.** The average computation MSE of the energy-greedy policy is upper bounded by  $1 + \ln 2$ , and the scaling law of the average computation MSE can be written as

$$\frac{\mathbb{E}[\text{MSE}]}{K} \sim 1, K \rightarrow \infty.$$

This policy is not a computation-effective one.

2) *Average Power Consumption*: From (18a), each sensor uses the same power  $P$  for information transmission, and we have the result below.

**Corollary 5.** The average power consumption of the energy-greedy policy is

$$\frac{\mathbb{E}[\text{PW}]}{K} = \lim_{K \rightarrow \infty} \frac{\mathbb{E}[\text{PW}]}{K} = P \neq 0.$$

This policy is not an energy-efficient one.



Comparing Corollaries 4 and 5 with Corollaries 2 and 3, the energy-greedy policy provides a better computation performance but has a lower energy efficiency than the channel-inversion policy when  $K$  is large. Therefore, there exists a design tradeoff between the computation effectiveness and the energy efficiency, and it is important to see whether there exists a Tx-Rx scaling policy that is both computation-effective and energy-efficient.

### C. The Existence of Computation-Effective and Energy-Efficient Policy

We introduce a new type of policy and study its scaling laws in terms of average computation MSE and average power consumption, which will further shed lights on the existence of computation-effective and energy-efficient policies and the scaling laws of the computation-optimal policy.

#### 1) Construction of A New Policy:

**Definition 6** (First- $\iota$  policy). A Tx-Rx scaling policy of the AirComp system is a first- $\iota$  policy if it satisfies:

- 1) the critical number is determined by a function, i.e.,  $i = \iota(K)$ , where  $\iota: \mathbb{N} \rightarrow \mathbb{N}$  and  $\iota(K) \leq K$ , and
- 2) the Rx-scaling factor  $a \in \mathcal{S}_i$ , and
- 3) the Tx-scaling factor  $b_k$  is given by (8),  $\forall k \in \{1, \dots, K\}$ .

**Remark 5.** Different from the optimal policy, where the critical number depends on all the values of the channel coefficients, a first- $\iota$  policy simply determines its critical number based on the total number of sensors  $K$ . The first  $i = \iota(K)$  sensors with the smallest channel coefficients use the maximum power for transmission.

2) *Scaling Law of Average Computation MSE:* For a first- $\iota$  policy, using Definition 6, it is clear that

$$\frac{1}{h_{\iota(K)+1}\sqrt{P}} \leq a \leq \frac{1}{h_{\iota(K)}\sqrt{P}}. \quad (31)$$

Taking the inequality (31) into (9), an upper bound of MSE is obtained as

$$\begin{aligned} \text{MSE} &\leq \sum_{k=1}^{\iota(K)} \left( \frac{h_k}{h_{\iota(K)+1}} - 1 \right)^2 + \frac{\sigma^2}{P} \frac{1}{h_{\iota(K)}^2} \\ &\leq \iota(K) + \frac{\sigma^2}{P} \frac{1}{U_{\iota(K)}}. \end{aligned} \quad (32)$$

and a lower bound of MSE is obtained as

$$\text{MSE} > \sum_{k=1}^{\iota(K)} \left( \frac{h_k}{h_{\iota(K)}} - 1 \right)^2 + \frac{\sigma^2}{P} \frac{1}{U_{\iota(K)+1}}. \quad (33)$$

Then, we have the following result.

**Theorem 3.** For a first- $\iota$  policy, the average computation MSE of the AirComp system has the following properties that

- 1) if  $\liminf_{K \rightarrow \infty} \iota(K) \leq 2$ ,

$$\limsup_{K \rightarrow \infty} \frac{\text{E}[\text{MSE}]}{K} \geq \frac{\sigma^2}{3P}, \quad (34)$$

- 2) if  $\liminf_{K \rightarrow \infty} \iota(K) > 2$  and  $\limsup_{K \rightarrow \infty} \iota(K)/K = c > 0$ ,

$$\limsup_{K \rightarrow \infty} \frac{\text{E}[\text{MSE}]}{K} \geq \frac{1}{c} \mu \left( \frac{c}{1+c} \right), \quad (35)$$

where

$$\mu(x) \triangleq \frac{x}{1-x} - \log(1-x) - 2\sqrt{\frac{x}{1-x}} \sin^{-1}(\sqrt{x}), \quad (36)$$

- 3) if  $\liminf_{K \rightarrow \infty} \iota(K) > 2$  and  $\lim_{K \rightarrow \infty} \iota(K)/K = 0$ ,

$$\frac{\text{E}[\text{MSE}]}{K} \sim \frac{\iota(K)}{K} + \frac{1}{\iota(K)}, K \rightarrow \infty. \quad (37)$$

*Proof.* See Appendix B. ■

For case 1) in (34), the average computation MSE does not converge to zero and such the first- $\iota$  policy is not computation-effective. From case 2) in (35), interestingly, we see that the energy-greedy policy in Definition 2, which has  $\limsup_{K \rightarrow \infty} \iota(K)/K = 1$ , is not computation-effective, since  $\limsup_{K \rightarrow \infty} \text{E}[\text{MSE}]/K \geq \mu(1/2) \approx 0.12 > 0$ . For case 3), from (37),  $\text{E}[\text{MSE}]/K$  converges to zero iff  $\iota(K) = o(K)$  and  $\liminf_{K \rightarrow \infty} \iota(K) \rightarrow \infty$ . Moreover, the average computation MSE has the decay rate of  $1/\sqrt{K}$  when  $\iota(K) \sim \sqrt{K}$ , while if  $\iota(K) = o(\sqrt{K})$  or  $1/\iota(K) = o(1/\sqrt{K})$ , we have  $1/\iota(K) \gg \iota(K)/K$  or  $1/\iota(K) \ll \iota(K)/K$  in (37), respectively, and the decay rate of the average computation MSE is larger than  $1/\sqrt{K}$ . Therefore, we have the following result.

**Proposition 3.** A first- $\iota$  policy is computation-effective iff  $\iota(K) = o(K)$  and  $\liminf_{K \rightarrow \infty} \iota(K) \rightarrow \infty$ . The largest decay rate of the average computation MSE achieved by first- $\iota$  policies is

$$\frac{\text{E}[\text{MSE}]}{K} \sim \frac{1}{\sqrt{K}}, K \rightarrow \infty,$$

when the critical-number function  $\iota(K) \sim \sqrt{K}$ .

From (15), the computation-optimal policy surely results in an average computation MSE no larger than that of a first- $\iota$  policy, we have the following result.

**Proposition 4.** The computation-optimal policy is a computation-effective one, and its average computation MSE has at least a decay rate of  $O(1/\sqrt{K})$  when  $K \rightarrow \infty$ .

3) *Scaling Law of Average Power Consumption:* From Definition 6, the power consumption of a first- $\iota$  policy is

$$\text{PW} = \iota(K)P + \frac{1}{a^2} \sum_{k=\iota(K)+1}^K \frac{1}{U_k}, a \in \mathcal{S}_{\iota(K)}. \quad (38)$$

We have the following result of its average power consumption.

**Theorem 4.** For a first- $\iota$  policy, the average power consumption of the AirComp system has the following properties that

- 1) if  $\liminf_{K \rightarrow \infty} \iota(K)/K = 1$ ,

$$\limsup_{K \rightarrow \infty} \frac{\text{E}[\text{PW}]}{K} = P, \quad (39)$$

TABLE I: Computation effectiveness and energy efficiency of AirComp Policies.

	Computation-Effective Policy	Energy-Efficient Policy
Benchmark Policy 1	✗	✓
Benchmark Policy 2	✗	✗
Computation-Optimal Policy	✓	✓
First- $\iota$ Policy with $\iota(K) = \sqrt{K}$	✓	✓
First- $\iota$ Policy with $\iota(K) = K/2$	✗	✗

2) if  $\limsup_{K \rightarrow \infty} \iota(K)/K = c' > 0$ ,

$$\limsup_{K \rightarrow \infty} \frac{E[\text{PW}]}{K} \geq c'P, \quad (40)$$

3) if  $\lim_{K \rightarrow \infty} \iota(K)/K = 0$ ,

$$O\left(\frac{\iota(K)}{K}\right) \leq \limsup_{K \rightarrow \infty} \frac{E[\text{PW}]}{K} \leq O\left(\frac{\iota(K) \log(K)}{K}\right). \quad (41)$$

*Proof.* See Appendix C. ■

From (41), a first- $\iota$  policy is energy-efficient as long as the critical number function  $\iota(K)$  has a lower divergence rate of  $K/\log(K)$ , and the decay rate of the average power consumption is no larger than  $O(\iota(K)/K)$ . Using Proposition 3 and Theorem 4, the following result can be obtained directly.

**Proposition 5.** The computation-effective first- $\iota$  policy achieving the minimum average computation MSE, i.e.,  $\iota(K) \sim \sqrt{K}$  when  $K \rightarrow \infty$ , is also energy-efficient, and its average power consumption has a decay rate between  $O(1/\sqrt{K})$  and  $O(\log(K)/\sqrt{K})$ .

Note that the scaling-law results of first- $\iota$  policies for average power consumption cannot provide insights directly into that of the computation-optimal policy. This is because the power consumption of the computation-optimal policy in (16) relies on the optimal critical number, which is determined by the sequence  $\{g_i\}$  in (11), and the statistics of the optimal critical number is difficult to analyze. Nevertheless, we numerically show that this policy is also an energy-efficient one in the following section. Therefore, by using the results obtained in this section, the computation effectiveness and energy efficiency of benchmark policies 1 and 2, computation-optimal policy, and two first- $\iota$  policies, i.e.,  $\iota(K) = \max\{1, \lfloor \sqrt{K} \rfloor\}$  and  $\iota(K) = \max\{1, \lfloor K/2 \rfloor\}$  are summarized in Table I.

## VI. NUMERICAL RESULTS

In this section, we numerically evaluate the average computation MSE and the average power consumption of the five Tx-Rx scaling policies of the AirComp system in Table I. Note that for the first- $\iota$  policies, the Rx-scaling factor is chosen as  $a = (1/h_{i(K)+1} + 1/h_{i(K)}) / (2\sqrt{P}) \in \mathcal{S}_{i(K)}$ . Unless otherwise stated, we set the sensor's transmission power  $P = 10$  and the receiving noise power  $\sigma^2 = 1$ . The average computation MSE,  $E[\text{MSE}]/K$ , and the average power consumption,  $E[\text{PW}]/K$ , induced by different policies are evaluated by using Monte Carlo simulation with  $10^6$  random channel realizations for calculating the average of  $\text{MSE}/K$

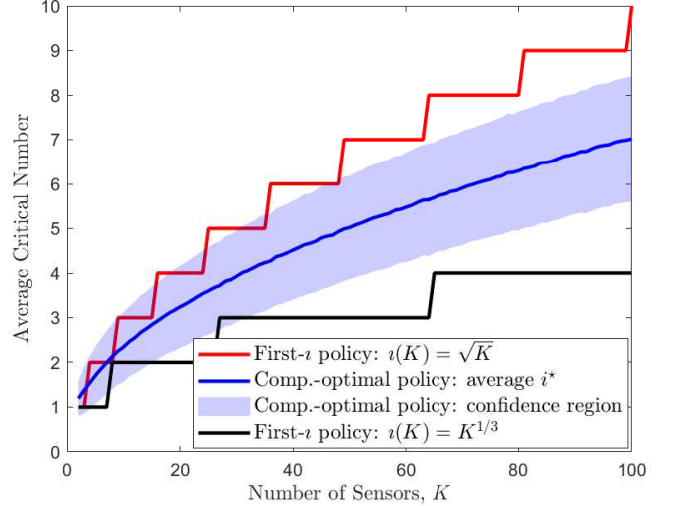


Fig. 4: The average critical number of the computation-optimal policy versus the number of sensors.

and  $\text{PW}/K$  based on (5) and (6), respectively. Also, the standard deviations of  $\text{MSE}/K$  and  $\text{PW}/K$  are evaluated as the confidence intervals of the average computation MSE and the average power consumption, respectively. In addition, for the computation-optimal policy, we also evaluate the average and the standard deviation of its critical number using Monte Carlo simulation with  $10^6$  points.

In Fig. 4, using Theorem 1, we plot the average critical number of the computation-optimal policy,  $E[i^*]$ , and the confidence region of  $i^*$  with different number of sensors  $K$ . We see both the average and the standard deviation of the critical number monotonically increase with  $K$ . Also, we plot the critical number of two first- $\iota$  policies with  $\iota(K) = \sqrt{K}$  and  $K^{1/3}$ , respectively. It shows that the scaling law of the average critical number of the computation-optimal policy has the properties that  $E[i^*] > K^{1/3}$  and  $E[i^*] < \sqrt{K}$ , when  $K > 10$ .

In Figs. 5 and 6, we plot the average computation MSE of the AirComp system and the standard deviation of  $\text{MSE}/K$ , respectively, with different policies in Table I, excluding benchmark policy 1, which has an infinite average computation MSE. We see that the computation-optimal policy has a remarkably lower average computation MSE than the other policies, and the policy with  $\iota(K) = \sqrt{K}$  is better than the one with  $\iota(K) = K/2$ , which is better than benchmark policy 2. Also, it can be observed that both the policy with  $\iota(K) = \sqrt{K}$  and the computation-optimal policy have average

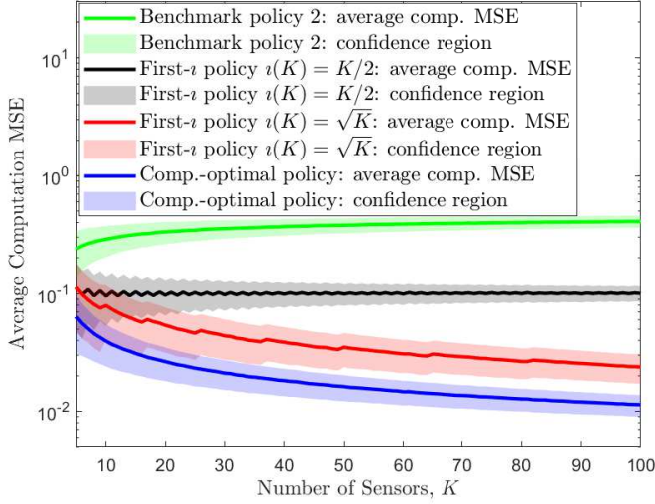


Fig. 5: The average computation MSE,  $E[\text{MSE}]/K$ , versus the number of sensors  $K$ .

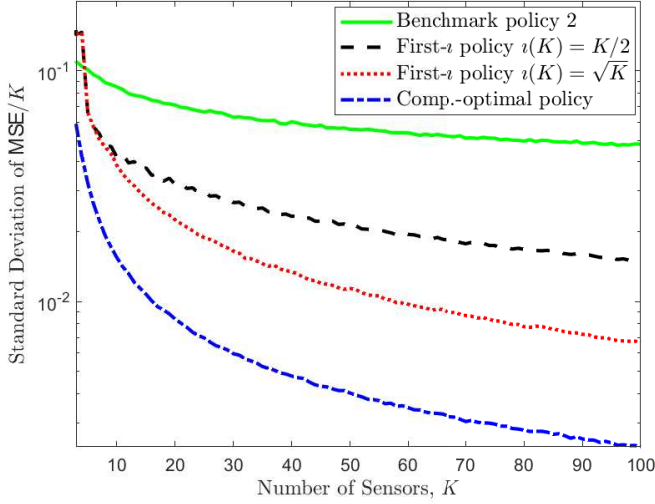


Fig. 6: The standard deviation of  $\text{MSE}/K$  versus the number of sensors  $K$ .

computation MSEs approaching to zero with the increasing  $K$ , which verifies Propositions 3 and 4, respectively. However, benchmark policy 2 and the policy with  $\iota(K) = K/2$  have average computation MSEs bounded away from zero and converges to 0.35 and 0.15, respectively, which are in line with Corollary 4 and Theorem 3. Nevertheless, all these four policies have diminishing standard deviations of  $\text{MSE}/K$  with the increasing  $K$ , which means that  $\text{MSE}/K$  converges to average computation MSE in probability when  $K \rightarrow \infty$ . Also, it is interesting to see that the policy with a lower average computation MSE has a smaller standard deviation when  $K > 10$ .

In Figs. 7 and 8, we plot the average power consumption of the AirComp system,  $E[\text{PW}]/K$  and the standard deviation

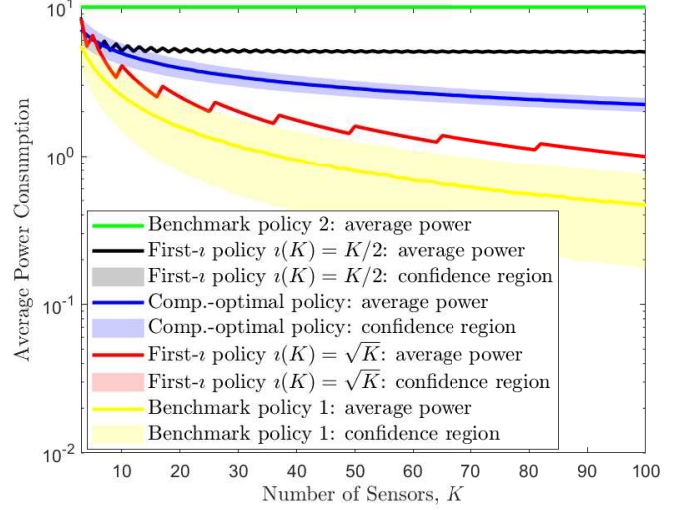


Fig. 7: The average power consumption,  $E[\text{PW}]/K$ , versus the number of sensors  $K$ .

of  $\text{PW}/K$ , respectively, with different policies in Table I. We see that benchmark policies 1 and 2 have the lowest and the highest power consumption, respectively. The policy with  $\iota(K) = \sqrt{K}$  and the computation-optimal policy both have average power consumption approaching to zero with the increasing  $K$ , which is in line with Propositions 5, and the former has a lower power consumption than the latter. Comparing Fig. 7 with Fig. 5, the computation-optimal policy has a better computation performance but a higher power consumption than the policy with  $\iota(K) = \sqrt{K}$ , which again shows the design tradeoff between computation effectiveness and energy efficiency. Also, we see the average power consumption of the policy with  $\iota(K) = K/2$  converges to 5, which is greater than  $P/3 = 3.3$ , which is in line with Theorem 4.

From Fig. 8, it can be observed that all the policies have diminished standard deviations of  $\text{PW}/K$  with the increasing  $K$ , which means that  $\text{PW}/K$  converges to average power consumption in probability when  $K \rightarrow \infty$ . It is interesting to see that the standard deviations of the first- $\iota$  policies are much smaller than that of the computation-optimal policy. This is mainly because the critical number is deterministic for the former and is stochastic for the latter. Recall that for a first- $\iota$  policy, the critical number does not rely on the random channel realizations, while the critical number of the computation-optimal policy heavily relies on the channel realizations, and thus has a large variance as shown in Fig. 4.

Fig. 9 shows the average power consumption of the computation-optimal policy with different transmission-power limit. We see that the average power consumption in all different cases decays to zero with the increasing number of sensors, which verifies that the policy is an energy-efficient one. Moreover, it seems that the decay rate does not rely too much on the transmission-power limit.

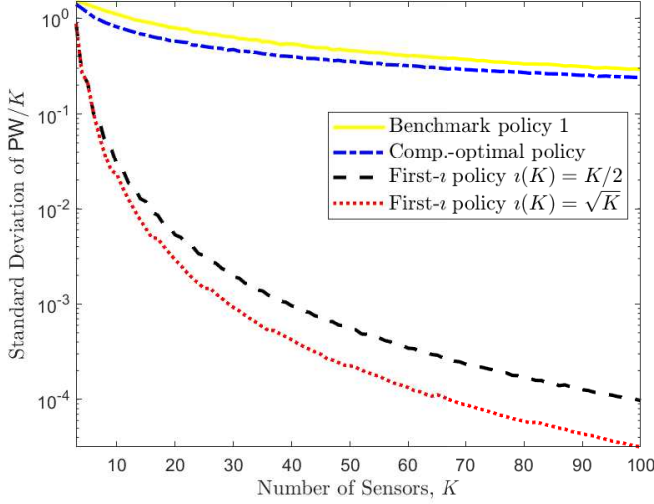


Fig. 8: The standard deviation of  $PW/K$  versus the number of sensors  $K$ , where benchmark policy 2 which has zero standard deviation of  $PW/K$ , is not included in the logarithmic-scale plot.

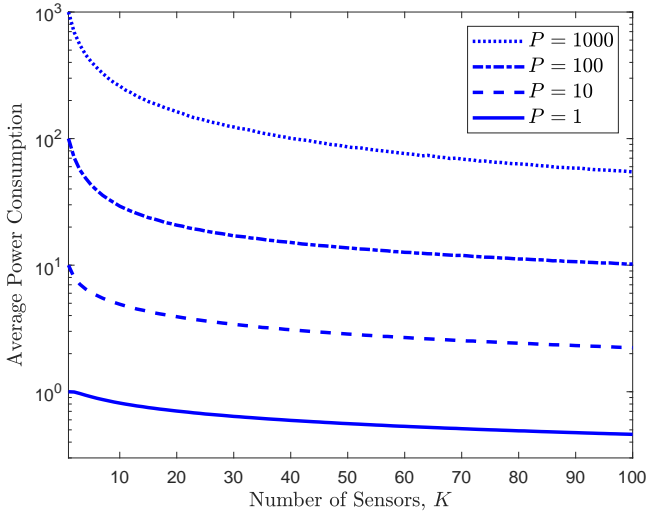


Fig. 9: The average critical number of the computation-optimal policy versus the number of sensors.

## VII. CONCLUDING REMARKS

In this work, we have derived the computation-optimal policy of the AirComp system, compared the AirComp system with the traditional MAC system, and investigated the ergodic performance of the AirComp system with different Tx-Rx scaling policies in terms of the number of sensors. Our results have shown that the computation-optimal policy has a vanishing average computation MSE and a vanishing average power consumption with the increasing number of sensors. By comparing the performance of the computation-optimal policy with that of the proposed first- $l$  policies, it reveals a design tradeoff between computation effectiveness and energy efficiency, which is very important for AirComp-

system implementation with practical computation accuracy and energy consumption constraints.

## APPENDIX A PROOF OF COROLLARY 3

The joint distribution function  $f(u_1, u_2, \dots, u_K)$  can be rewritten as

$$f(u_1, u_2, \dots, u_K) = f(u_2, \dots, u_K | u_1) f(u_1). \quad (\text{A.1})$$

Since the average power in (28) does not rely on the order of the largest  $K - 1$  channel power gains,  $U_k, k > 1$ , in the rest of the proof, we treat  $\{U_k\}$  as  $K$  independent exponential random variables that  $U_k, \forall k > 1$ , is no smaller than  $U_1$ . In this sense, the conditional joint distribution in (A.1) can be rewritten as

$$\begin{aligned} & f(u_2, \dots, u_K | u_1, \Xi_1) \\ &= f(u_2 | u_1, \Xi_1) f(u_3 | u_1, \Xi_1) \cdots f(u_K | u_1, \Xi_1) \\ &= \begin{cases} e^{(K-1)u_1 - (u_2 + \dots + u_K)}, & u_2, \dots, u_K > u_1 \\ 0, & \text{else.} \end{cases} \end{aligned}$$

where  $\Xi_1$  is the event that  $U_1 \leq U_2, \dots, U_K$ , and  $f(u_1)$  given in (26) can be denoted as  $f(u_1 | \Xi_1)$ .

Then, it follows that

$$\begin{aligned} & \mathbb{E} \left[ \sum_{k=2}^K \frac{U_1}{U_k} \middle| \Xi_1 \right] \\ &= \int_{u_1 > 0} \int_{u_2 > u_1} \cdots \int_{u_K > u_1} \sum_{k=2}^K \frac{u_1}{u_k} f(u_1 | \Xi_1) \\ & \quad f(u_2, \dots, u_K | u_1, \Xi_1) du_K \cdots du_1 \\ &= \int_{u_1 > 0} \int_{u_2 > u_1} \cdots \int_{u_K > u_1} \sum_{k=2}^K \frac{u_1}{u_k} K \exp \left( - \sum_{k=1}^K u_k \right) \\ & \quad du_K \cdots du_1 \\ &= K(K-1) \int_{u_1 > 0} \int_{u_2 > u_1} \frac{u_1}{u_2} \exp \left( -(K-1)u_1 - u_2 \right) du_2 du_1 \\ &= K(K-1) \int_{u_2 > 0} \int_0^{u_2} \frac{u_1}{u_2} \exp \left( -(K-1)u_1 - u_2 \right) du_1 du_2 \\ &= \frac{K}{K-1} \int_0^\infty \frac{e^{-u_2}}{u_2} \left( 1 - (1 + (K-1)u_2) e^{-(K-1)u_2} \right) du_2 \\ &= \frac{K \ln K - (K-1)}{K-1}. \end{aligned} \quad (\text{A.2})$$

Corollary 3 is obtained by taking (A.2) into (28).

APPENDIX B  
PROOF OF THEOREM 3

From (32), an upper bound of the average computation MSE is derived as

$$\begin{aligned} \frac{\mathbb{E}[\text{MSE}]}{K} &\leq \frac{\iota(K)}{K} + \frac{\sigma^2}{PK} \mathbb{E} \left[ \frac{1}{U_{\iota(K)}} \right] \\ &= \frac{\iota(K)}{K} + \frac{\sigma^2}{PK} \mathbb{E} \left[ \frac{1}{\sum_{j=1}^{\iota(K)} \frac{Z_j}{K-j+1}} \right] \end{aligned} \quad (\text{A.3})$$

$$\begin{aligned} &\leq \frac{\iota(K)}{K} + \frac{\sigma^2}{PK} \mathbb{E} \left[ \frac{K}{\sum_{j=1}^{\iota(K)} Z_j} \right] \\ &= \frac{\iota(K)}{K} + \frac{\sigma^2}{P} \frac{1}{\iota(K) - 1}, \end{aligned} \quad (\text{A.4})$$

where (A.3) is due to the property that for  $K$  random samples from an exponential distribution with parameter 1, the order statistics  $U_i$  for  $i = 1, 2, 3, \dots, K$  each has the distribution [35]

$$U_i \stackrel{d}{=} \sum_{j=1}^i \frac{Z_j}{K-j+1},$$

and  $Z_j, j = 1, \dots, i$  are i.i.d. standard exponential random variables. (A.4) is due to the fact that  $\frac{1}{\sum_{j=1}^{\iota(K)} Z_j}$  follows inverse gamma distribution with mean  $\frac{1}{\iota(K)-1}$ .

From (33), a lower bound of the average computation MSE is derived as

$$\frac{\mathbb{E}[\text{MSE}]}{K} \geq \frac{1}{K} \sum_{k=1}^{\iota(K)} \mathbb{E} \left[ \left( \frac{h_k}{h_{\iota(K)}} - 1 \right)^2 \right] + \mathbb{E} \left[ \frac{\sigma^2}{PK} \frac{1}{U_{\iota(K)+1}} \right]. \quad (\text{A.5})$$

Then, we derive the lower bounds of the first and second terms on the right-hand side (RHS) of (A.5) using the following technical lemma.

**Lemma 3a.** *Let  $X_1, X_2, \dots, X_K$  be a random sample from the standard exponential distribution, and let  $X_{(1)}, X_{(2)}, \dots, X_{(K)}$  denote the order statistics obtained from this sample. The expectation of the ratio  $\frac{X_{(i)}}{X_{(j)}}$  has the inequality*

$$\mathbb{E} \left[ \frac{X_{(i)}}{X_{(j)}} \right] < \frac{(i+1)}{(K-i+1)} \frac{K}{(j-2)}, \forall j > 2.$$

*Proof.* It can be derived that

$$\mathbb{E} \left[ \frac{X_{(i)}}{X_{(j)}} \right] \leq \sqrt{\mathbb{E}[X_{(i)}] \mathbb{E} \left[ \frac{1}{X_{(j)}} \right]} \quad (\text{A.6})$$

$$\begin{aligned} &\leq \sqrt{\frac{(i^2+i)}{(K-i+1)^2} \frac{K^2}{(j-1)(j-2)}} \quad (\text{A.7}) \\ &< \frac{(i+1)}{(K-i+1)} \frac{K}{(j-2)}, \forall j > 2. \end{aligned}$$

and (A.6) is due to the Cauchy-Schwarz inequality, i.e.,  $\mathbb{E}[|XY|] \leq \sqrt{\mathbb{E}[X^2]\mathbb{E}[Y^2]}$ . (A.7) is obtained by using the inequalities

$$\frac{1}{K} \sum_{j=1}^i Z_j \preceq X_i \stackrel{d}{=} \sum_{j=1}^i \frac{Z_j}{K-j+1} \preceq \frac{1}{K-i+1} \sum_{j=1}^i Z_j, \forall i, \quad (\text{A.8})$$

and the property that  $\sum_{j=1}^i Z_j$  and  $\frac{1}{\sum_{j=1}^i Z_j}$  follows the gamma distribution  $\text{Gamma}(i, 1)$  and the inverse gamma distribution  $\text{Inv} - \text{Gamma}(i, 1)$ , respectively. ■

For the second term on the RHS of (A.5), using the Jensen's inequality and (A.8), it is easy to have

$$\mathbb{E} \left[ \frac{\sigma^2}{PK} \frac{1}{U_{\iota(K)+1}} \right] \geq \frac{\sigma^2}{PK} \frac{K - \iota(K)}{\iota(K) + 1}. \quad (\text{A.9})$$

Thus, if  $\liminf_{K \rightarrow \infty} \iota(K) \leq 2$ ,  $\limsup_{K \rightarrow \infty} \frac{\mathbb{E}[\text{MSE}]}{K} \geq \frac{\sigma^2}{PK} \frac{K - \liminf_{K \rightarrow \infty} \iota(K)}{\liminf_{K \rightarrow \infty} \iota(K) + 1} \geq \frac{\sigma^2}{3P}, K \rightarrow \infty$ , completing the proof of (34). In the following, we assume that  $\liminf_{K \rightarrow \infty} \iota(K) > 2$ .

For the first term on the RHS of (A.5), we have the following inequality

$$\begin{aligned} \mathbb{E} \left[ \left( \frac{h_k}{h_{\iota(K)}} - 1 \right)^2 \right] &\geq \left( 1 - \sqrt{\mathbb{E} \left[ \frac{U_k}{U_{\iota(K)}} \right]} \right)^2 \quad (\text{A.10}) \\ &\geq \left( \left[ 1 - \sqrt{\frac{K}{K-k+1} \frac{k+1}{\iota(K)-2}} \right]^+ \right)^2, \forall \iota(K) > 2, k \leq \iota(K). \end{aligned} \quad (\text{A.11})$$

where (A.10) is due to the Jensen's inequality and the convexity of the function  $(1-\sqrt{x})^2$ , (A.11) is obtained by Lemma 3a, and  $[x]^+ \triangleq \max\{x, 0\}$ .

Therefore, it can be obtained that

$$\begin{aligned} &\frac{1}{K} \sum_{k=1}^{\iota(K)} \mathbb{E} \left[ \left( \frac{h_k}{h_{\iota(K)}} - 1 \right)^2 \right] \\ &\geq \frac{1}{K} \sum_{k=1}^{\iota(K)} \left( \left[ 1 - \sqrt{\frac{K}{K-k+1} \frac{k+1}{\iota(K)-2}} \right]^+ \right)^2, \forall \iota(K) > 2 \end{aligned} \quad (\text{A.12})$$

$$\geq \frac{1}{K} \sum_{k=2}^{\iota(K)} \left( \left[ 1 - \sqrt{\frac{K}{K-k} \frac{k}{\iota(K)-2}} \right]^+ \right)^2 \quad (\text{A.13})$$

$$\geq \frac{1}{K} \frac{1}{\iota(K)-2} \sum_{k=2}^{g(K)} \left( \left[ \sqrt{\frac{\iota(K)-2}{K}} - \sqrt{\frac{k}{1-\frac{k}{K}}} \right]^+ \right)^2$$

APPENDIX C  
PROOF OF THEOREM 4

$$\begin{aligned} &\geq \frac{1}{\frac{\iota(K)-2}{K}} \sum_{k=2}^{g(K)} \left( \sqrt{\frac{\frac{g(K)}{K}}{1-\frac{g(K)}{K}}} - \sqrt{\frac{\frac{k}{K}}{1-\frac{k}{K}}} \right)^2 \frac{1}{K} \\ &= \frac{1}{\frac{\iota(K)-2}{K}} \left( \int_0^{\frac{g(K)}{K}} \left( \sqrt{\frac{\frac{g(K)}{K}}{1-\frac{g(K)}{K}}} - \sqrt{\frac{x}{1-x}} \right)^2 dx + o\left(\frac{1}{K}\right) \right) \end{aligned} \quad (\text{A.14})$$

$$= \frac{1}{\frac{\iota(K)-2}{K}} \left( \mu\left(\frac{g(K)}{K}\right) \right) + o\left(\frac{1}{\iota(K)}\right) \quad (\text{A.15})$$

where

$$g(K) = \left\lfloor \frac{\iota(K) - 2}{1 + (\iota(K) - 2)/K} \right\rfloor,$$

and  $\mu(x)$  is defined in (36) and it can be proved that

$$\mu(x) = \frac{1}{6}x^2 + o(x^3), x \rightarrow 0.$$

(A.13) is due to  $K - k + 1 > K - k - 1^6$  and is obtained by replacing  $(k + 1)$  with  $k$ , (A.14) is due to the facts that  $g(K)/K < 1/2$  and the function  $\sqrt{x/(1-x)}$  is monotonic and bounded in  $[0, 1/2]$ , and is obtained by using Riemann integral to approximate Riemann sum when  $K$  is large.

Assuming that  $\limsup_{K \rightarrow \infty} \frac{\iota(K)}{K} = c \neq 0$ , from (A.15), we have

$$\begin{aligned} \limsup_{K \rightarrow \infty} \frac{\mathbb{E}[\text{MSE}]}{K} &\geq \limsup_{K \rightarrow \infty} \frac{1}{K} \sum_{k=1}^{\iota(K)} \mathbb{E} \left[ \left( \frac{h_k}{h_{\iota(K)}} - 1 \right)^2 \right] \\ &\geq \frac{1}{c} \mu\left(\frac{c}{1+c}\right), \end{aligned}$$

completing the proof of (35).

Assuming that  $\lim_{K \rightarrow \infty} \frac{\iota(K)}{K} = 0$ , we have

$$\mu(g(K)/K) = \frac{1}{6} \left( \frac{\iota(K)}{K} \right)^2 + o\left( \left( \frac{\iota(K)}{K} \right)^3 \right) + o\left( \frac{1}{\iota(K)} \right). \quad (\text{A.16})$$

Taking (A.16) into (A.15) and jointly using (A.9) in (A.5), it can be obtained that

$$\frac{\mathbb{E}[\text{MSE}]}{K} \geq \frac{1}{6} \frac{\iota(K)}{K} + \frac{\sigma^2}{P} \frac{1}{\iota(K)} + o\left(\frac{\iota(K)}{K}\right) + o\left(\frac{1}{\iota(K)}\right), K \rightarrow \infty. \quad (\text{A.17})$$

From the upper and lower bounds (A.4) and (A.17), (37) can be obtained.

<sup>6</sup>Note that here we assume that  $\iota(K) + 1 < K$  in (A.12). For the case that  $\iota(K) + 1 \geq K$ , the summation in (A.12) can be rewritten as  $\sum_{k=1}^{\iota(K)-2} \left( \left[ 1 - \sqrt{\frac{K}{K-k+1} \frac{k+1}{\iota(K)-2}} \right]^+ \right)^2 + \sum_{k=\iota(K)-1}^{\iota(K)} \left( \left[ 1 - \sqrt{\frac{K}{K-k+1} \frac{k+1}{\iota(K)-2}} \right]^+ \right)^2$ . Following the similar steps of the  $\iota(K) + 1 < K$  case, this one has the same asymptotic results as the  $\iota(K) + 1 < K$  case and the detailed analysis is omitted for brevity.

From (38), an upper bound and a lower bound of the average power consumption can be obtained as

$$\frac{\mathbb{E}[\text{PW}]}{K} \leq \frac{P}{K} \left( \iota(K) + \sum_{k=\iota(K)+1}^K \mathbb{E} \left[ \frac{h_{\iota(K)+1}^2}{h_k^2} \right] \right) \quad (\text{A.18})$$

$$\frac{\mathbb{E}[\text{PW}]}{K} \geq \frac{P}{K} \iota(K). \quad (\text{A.19})$$

For the case that  $\liminf_{K \rightarrow \infty} \iota(K) = K$ , using (A.19) and the fact that  $\text{PW}/K \leq P$ , we have  $\limsup_{K \rightarrow \infty} \frac{\mathbb{E}[\text{PW}]}{K} = P$ , which completes the proof of (39). For the case that  $\limsup_{K \rightarrow \infty} \iota(K)/K = c' \neq 0$ , using (A.19), we have  $\limsup_{K \rightarrow \infty} \frac{\mathbb{E}[\text{PW}]}{K} \geq c'P$ , which completes the proof of (40).

For the case that  $\limsup_{K \rightarrow \infty} \iota(K)/K = 0$ , using (A.18) and (A.19), we further have

$$\frac{\mathbb{E}[\text{PW}]}{K} < \frac{P}{K} \left( \iota(K) + \sum_{k=\iota(K)+1}^K \frac{(\iota(K) + 2)}{(K - \iota(K)) (k - 2)} \right), \forall \iota(K) < K \quad (\text{A.20})$$

$$\begin{aligned} &< \frac{P}{K} \left( \iota(K) + \frac{(\iota(K) + 2)K}{(K - \iota(K))} \sum_{k=1}^K \frac{1}{k} \right) \\ &= P \left( \frac{\iota(K)}{K} + \frac{\iota(K) + 2}{K - \iota(K)} O(\log(K)) \right), K \rightarrow \infty \quad (\text{A.21}) \\ &= O\left( \frac{\iota(K) \log(K)}{K} \right), K \rightarrow \infty, \end{aligned}$$

and

$$\frac{\mathbb{E}[\text{PW}]}{K} \geq \frac{P}{K} \iota(K) = O\left( \frac{\iota(K)}{K} \right), K \rightarrow \infty,$$

where (A.20) is a consequence of Lemma 3a (A.21) is due to the property of the harmonic series, which completes the proof of (41).

REFERENCES

- [1] X. Wu, X. Zhu, G.-Q. Wu, and W. Ding, "Data mining with big data," *IEEE Trans. Knowl. Data Eng.*, vol. 26, no. 1, pp. 97–107, 2013.
- [2] D. Inc, *Data Never Sleeps 6.0*, 2018. [Online]. Available: <https://www.domo.com/learn/data-never-sleeps-6>
- [3] Forbes, *How Much Data Do We Create Every Day? The Mind-Blowing Stats Everyone Should Read*, 2018. [Online]. Available: <https://www.forbes.com/sites/bernardmarr/2018/05/21/how-much-data-do-we-create-every-day-the-mind-blowing-stats-everyone-should-read>
- [4] R. C. Buck, "Approximate complexity and functional representation," *J. Math. Anal. Appl.*, vol. 70, pp. 280–298, 1979.
- [5] M. Goldenbaum and S. Stanczak, "Robust analog function computation via wireless multiple-access channels," *IEEE Trans. Commun.*, vol. 61, no. 9, pp. 3863–3877, Sep. 2013.
- [6] M. Goldenbaum, H. Boche, and S. Stanczak, "Harnessing interference for analog function computation in wireless sensor networks," *IEEE Trans. Signal Process.*, vol. 61, no. 20, pp. 4893–4906, Oct 2013.
- [7] Z. Kallenborn, *The era of the drone swarm is coming*, 2018. [Online]. Available: <https://mwi.usma.edu/era-drone-swarm-coming-need-ready/>
- [8] US Department of Transportation, *How an Automated Car Platoon Works*, 2017. [Online]. Available: <https://www.volpe.dot.gov/news/how-automated-car-platoon-works>
- [9] F. Molinari, S. Stanczak, and J. Raisch, "Exploiting the superposition property of wireless communication for average consensus problems

- in multi-agent systems,” in *Proc. European Control Conference (ECC)*, 2018, pp. 1766–1772.
- [10] G. Zhu, D. Liu, Y. Du, C. You, J. Zhang, and K. Huang, “Towards an intelligent edge: Wireless communication meets machine learning,” *arXiv preprint arXiv:1809.00343*, 2018.
- [11] M. M. Amiri and D. Gunduz, “Machine learning at the wireless edge: Distributed stochastic gradient descent over-the-air,” *arXiv preprint arXiv:1901.00844*, 2019.
- [12] J.-H. Ahn, O. Simeone, and J. Kang, “Wireless federated distillation for distributed edge learning with heterogeneous data,” *arXiv preprint arXiv:1907.02745*, 2019.
- [13] M. Goldenbaum, H. Boche, and S. Staczak, “Nomographic gossiping for f-consensus,” in *Proc. IEEE WiOpt*, May 2012, pp. 130–137.
- [14] O. Abari, H. Rahul, and D. Katabi, “Over-the-air function computation in sensor networks,” *arXiv preprint*, 2016. [Online]. Available: <https://arxiv.org/pdf/1612.02307.pdf>
- [15] G. Zhu and K. Huang, “Mimo over-the-air computation for high-mobility multimodal sensing,” *IEEE Internet Things J.*, vol. 6, no. 4, pp. 6089–6103, Aug 2019.
- [16] X. Li, G. Zhu, Y. Gong, and K. Huang, “Wirelessly powered data aggregation for iot via over-the-air function computation: Beamforming and power control,” *IEEE Trans. Wireless Commun.*, vol. 18, no. 7, pp. 3437–3452, Jul. 2019.
- [17] M. Goldenbaum and S. Staczak, “On the channel estimation effort for analog computation over wireless multiple-access channels,” *IEEE Wireless Commun. Lett.*, vol. 3, no. 3, pp. 261–264, June 2014.
- [18] T. Berger, Zhen Zhang, and H. Viswanathan, “The ceo problem,” *IEEE Trans. Inf. Theory*, vol. 42, no. 3, pp. 887–902, May 1996.
- [19] C. Wang, A. S. Leong, and S. Dey, “Distortion outage minimization and diversity order analysis for coherent multiaccess,” *IEEE Trans. Signal Process.*, vol. 59, no. 12, pp. 6144–6159, Dec 2011.
- [20] J. Xiao, S. Cui, Z. Luo, and A. J. Goldsmith, “Linear coherent decentralized estimation,” *IEEE Trans. Signal Process.*, vol. 56, no. 2, pp. 757–770, Feb 2008.
- [21] F. Jiang, J. Chen, and A. L. Swindlehurst, “Estimation in phase-shift and forward wireless sensor networks,” *IEEE Trans. Signal Process.*, vol. 61, no. 15, pp. 3840–3851, Aug 2013.
- [22] —, “Optimal power allocation for parameter tracking in a distributed amplify-and-forward sensor network,” *IEEE Trans. Signal Process.*, vol. 62, no. 9, pp. 2200–2211, May 2014.
- [23] A. S. Leong, S. Dey, G. N. Nair, and P. Sharma, “Power allocation for outage minimization in state estimation over fading channels,” *IEEE Trans. Signal Process.*, vol. 59, no. 7, pp. 3382–3397, Jul. 2011.
- [24] J. H. Braslavsky, R. H. Middleton, and J. S. Freudenberg, “Feedback stabilization over signal-to-noise ratio constrained channels,” *IEEE Trans. Autom. Control*, vol. 52, no. 8, pp. 1391–1403, Aug 2007.
- [25] W. Liu, P. Popovski, Y. Li, and B. Vucetic, “Wireless networked control systems with coding-free data transmission for industrial IoT,” *arXiv preprint*, 2019. [Online]. Available: <https://arxiv.org/pdf/1907.13297.pdf>
- [26] M. Gastpar, “Uncoded transmission is exactly optimal for a simple Gaussian “Sensor” network,” *IEEE Trans. Info. Theory*, vol. 54, no. 11, pp. 5247–5251, Nov. 2008.
- [27] M. Gastpar and M. Vetterli, “Power, spatio-temporal bandwidth, and distortion in large sensor networks,” *IEEE J. Sel. Areas Commun.*, vol. 23, no. 4, pp. 745–754, Apr. 2005.
- [28] M. Gastpar and M. Vetterli, “Source-channel communication in sensor networks,” in *Proc. ACM/IEEE IPSN*, 2003, pp. 162–177.
- [29] P. Viswanath, D. N. C. Tse *et al.*, “Sum capacity of the vector gaussian broadcast channel and uplink-downlink duality,” *IEEE Trans. Inf. Theory*, vol. 49, no. 8, pp. 1912–1921, 2003.
- [30] R. Zhang, S. Cui, and Y. Liang, “On ergodic sum capacity of fading cognitive multiple-access and broadcast channels,” *IEEE Trans. Inf. Theory*, vol. 55, no. 11, pp. 5161–5178, Nov 2009.
- [31] Z. Ding, Z. Yang, P. Fan, and H. V. Poor, “On the performance of non-orthogonal multiple access in 5g systems with randomly deployed users,” *IEEE Signal Process. Lett.*, vol. 21, no. 12, pp. 1501–1505, 2014.
- [32] E. A. Jorswieck, B. Ottersten, A. Sezgin, and A. Paulraj, “Guaranteed performance region in fading orthogonal space-time coded broadcast channels,” in *Proc. IEEE ISIT*, 2007, pp. 96–100.
- [33] X. Cao, G. Zhu, J. Xu, and K. Huang, “Optimal power control for over-the-air computation in fading channels,” *arXiv preprint*, 2019. [Online]. Available: <https://arxiv.org/pdf/1906.06858.pdf>
- [34] G. Zhu, S. Ko, and K. Huang, “Inference from randomized transmissions by many backscatter sensors,” *IEEE Trans. Wireless Commun.*, vol. 17, no. 5, pp. 3111–3127, May 2018.
- [35] B. C. Arnold, N. Balakrishnan, and H. N. Nagaraja, *A first course in order statistics*. Siam, 1992, vol. 54.